Macromolecular Materials and Engineering

Biofabrication of gelatin tissue scaffolds with uniform pore size via microbubble assembly

--Manuscript Draft--

Manuscript Number:	mame.201900394R1
Full Title:	Biofabrication of gelatin tissue scaffolds with uniform pore size via microbubble assembly
Article Type:	Full Paper
Section/Category:	
Keywords:	gelatin; scaffolds; forming; porosity; microbubbles
Corresponding Author:	Mohan Edirisinghe University College London London, UNITED KINGDOM
Corresponding Author Secondary Information:	
Corresponding Author's Institution:	University College London
Corresponding Author's Secondary Institution:	
First Author:	Cem Bayram
First Author Secondary Information:	
Order of Authors:	Cem Bayram
	Xinyue Jiang
	Merve Gultekinoglu
	Sukru Ozturk
	Kezban Ulubayram
	Mohan Edirisinghe
Order of Authors Secondary Information:	
Abstract:	Gelatin is widely used as an essential natural material in biomaterials science due to its resemblance to native extracellular matrix, and holds great potential in tissue engineering research. However, the control of pore size and uniform porosity remains as an important challenge in gelatin scaffolds. The precise control in building blocks of tissue scaffolds without any additional porogen is possible with costly equipment and techniques, though some pre-requirements for polymeric material, such as photo-polymerizability or sintering ability,may be needed prior to construction. Herein, a method for the fabrication of gelatin scaffolds with homogenous porosity using simple T-junction microfluidics is described. The size of the microbubbles were precisely controlled with 5% deviation from the average. Porous gelatin scaffolds were obtained by building-up the monodispersed microbubbles in dilute crosslinker solutions. After crosslinking, pore size of the resultant five scaffold groups were precisely controlled as 135±11, 193±11, 216±9, 231±5 and 250±12 μm. Porosity ratios above 65% were achieved in every sample group. Structures support high cell adhesion, viability and migration through the porous network via interconnectivity. Our study offers a practical and economical approach for the preparation of porous gelatin scaffolds with homogenous porosity which can be utilized in diverse tissue engineering applications.
Additional Information:	
Question	**Response**
Please submit a plain text version of your cover letter here.	

	Please find our revised version. 23rd June 2019 Dr David Huesmann Editor Macromolecular Materials and Engineering Dear David, Enclosed please kindly find the original research manuscript entitled “Biofabrication of gelatin tissue scaffolds with uniform pore size via microbubble assembly” which Cem Bayram, Xinyue Jiang, Merve Gultekinoglu, Şükrü Öztürk, Kezban Ulubayram and I would like you to consider for publication in Macromolecular Materials and Engineering. In our study, we demonstrate a practical approach to fabricate 3D gelatin tissue scaffolds with uniform, interconnective pores. The size of the microbubbles were precisely controlled with 5% deviation from the average. Fabrication of microbubbles was carried out through a simple T-junction type microfluidic system with nitrogen gas and gelatin solution without any surfactant and resulting microbubbles were collected at the end of the outlet channel and cross-linked in dilute glutaraldehyde to form 3D biopolymeric foam structures. The entire fabrication is a one-step process and free from any additional porogen materials. Factors affecting the microbubble size were investigated in the first part and the tissue scaffolds with different pore sizes were characterized in detail, including cell culture studies. We refer to a good compliment of related papers published in the journal. The manuscript is prepared according to the author guidelines of Macromolecular Materials and Engineering. We hope that you and the referees’ like this manuscript which we think will be of immense readership of “Macromolecular Materials and Engineering” as we show a tunable approach to fabricate highly monodisperse gelatin microbubbles and assemble them into a biocompatible and degradable tissue scaffold for diverse applications. Yours sincerely Mohan Prof. Mohan Edirisinghe University College London (Corresponding author)
Do you or any of your co-authors have a conflict of interest to declare?	No. The authors declare no conflict of interest.

WILEY-VCH

Biofabrication of gelatin tissue scaffolds with uniform pore size via microbubble assembly

*Cem Bayram†, Xinyue Jiang†, Merve Gultekinoglu, Sukru Ozturk, Kezban Ulubayram and Mohan Edirisinghe**

Dr. Cem Bayram
Advanced Technologies Application and Research Center, Hacettepe University, Ankara, Turkey.

Dr. Xinyue Jiang
Department of Mechanical Engineering, University College London (UCL), London WC1E 7JE, UK.

Dr. Merve Gultekinoglu, Sukru Ozturk and Prof. Dr. Kezban Ulubayram
Department of Basic Pharmaceutical Sciences, Faculty of Pharmacy, Hacettepe University, Turkey.

Prof. Dr. Mohan Edirisinghe
Department of Mechanical Engineering, University College London (UCL), London WC1E 7JE, UK

† CB and XJ contributed equally to this work.

*Corresponding author ME- m.edirisinghe@ucl.ac.uk

Keywords: biofabrication, tissue scaffold, microbubbles, gelatin

Abstract

Gelatin is widely used as an essential natural material in biomaterials science due to its resemblance to native extracellular matrix, and holds great potential in tissue engineering research. However, the control of pore size and uniform porosity remains as an important challenge in gelatin scaffolds. The precise control in building blocks of tissue scaffolds without any additional porogen is possible with costly equipment and techniques, though some pre-requirements for polymeric material, such as photo-polymerizability or sintering ability,may be needed prior to construction. Herein, a method for the fabrication of gelatin scaffolds with homogenous porosity using simple T-junction microfluidics is described. The size of the microbubbles were precisely controlled with 5% deviation from the average. Porous gelatin scaffolds were obtained by building-up the monodispersed microbubbles in dilute crosslinker solutions. The effect of crosslinker density on pore diameter was also investigated. After crosslinking, pore size of the resultant five scaffold groups were precisely controlled as 135±11, 193±11, 216±9, 231±5 and 250±12 μm. Porosity ratios above 65% were achieved in every sample group. According to the cell culture experiments, structures support high cell adhesion, viability and migration through the porous network via interconnectivity. Our study offers a practical and economical approach for the preparation of porous gelatin scaffolds with homogenous porosity which can be utilized in diverse tissue engineering applications.

1. Introduction

Tissue engineering is a joint approach with a vast variety of disciplines from medicine to engineering contributing to its developments and holds a great potential for restoring the functions of the tissues and organs. Tissue regeneration from bench to bedside is a holistic method combining materials science, cell culture, engineering and surgery with additional support from other disciplines such as molecular biology, statistics etc.[1,2] Tissue scaffolds are one of the three elements of tissue engineering, besides cells and growth factors, providing a support material for cell adhesion and proliferation before histogenesis. The general characteristics of tissue scaffolds are well defined and can be summarized as biodegradation capability to non-toxic substances (bioresorbability), bearing loading conditions comparable to related tissue and having interconnected porosity.[3,4] The latter is a vital feature since it allows both nutrient flow and cell migration throughout the 3D structure, neovascularization and contributes to mechanical properties of the scaffold.[5] In addition, the porous structure can facilitate integration between the scaffold and tissue. Generally, it is accepted that the ideal pore is between 100 – 400 μm and high porosity (>50%) with maximum interconnectivity is required.[6-9] However, uneven distribution of pore size results in inhomogeneity in porosity and mechanical properties all the way along the scaffold.[10,11] Phase separation[12], gas foaming[13], salt leaching[14] and freeze drying[15] techniques are conventional porous scaffold fabrication methods in which all of the porosity and scaffold architecture cannot be controlled precisely. Besides, rapid prototyping techniques such as 3D printing,[16] selective laser sintering,[17] stereolitography[18] or fused deposition modelling,[19] which emerged in the last decade have the capability to control accurate pore positioning, however each of the techniques is still costly compared to conventional techniques. Moreover, the scaffold material is required to have some other special abilities in most rapid prototyping techniques such as photo-polymerizability,

pseudoplasticity, sintering ability etc., restricting each method with limited compatible materials.

Microbubbles of polymeric materials are essential for a broad range of applications, such as drug discovery, cell encapsulation, medical diagnostics and more recently fabrication of porous biomaterials.[20-23] It is possible to overcome the disadvantages of both conventional and rapid prototyping methods with recently developed versatile and robust techniques of microbubble generation. Bottom-up fabrication approach of tissue scaffolds with microbubbles allows precise control of a very narrow pore size distribution.[24] The technique is simple, fast and does not require a template or a complex setup. Gas trapped monodispersed microbubbles of tissue scaffold material can be obtained via microfluidic setups in a single step. Our previous studies showed that the generation of bubbles and porous membranes of various polymeric materials with narrow size distribution via a T-junction microfluidic device is possible and promising for tissue scaffold fabrication.[20,25] In a T-type junction, continuous and disperse phases meet at a point where the two channels are perpendicular to each other. The disperse phase penetrates inside the main flow and the continuous phase pushes the droplet downstream creating a neck along the channel. After the necking part elongates up to a final length, droplets detach from the disperse phase and individually travel along the main channel. The process repeats itself as the disperse and continuous phases enter alternately into the main channel, thus gas entrapped monodispersed microbubbles can be collected from the outlet flow when gas is used as the continuous phase.[26,27]

The use of a microfluidic set up for three-dimensional tissue scaffolds begins with Chung et al.'s work,[28] where a flow-focusing device was used for the fabrication of calcium chloride cross-linked alginate bubbles. The study emphasized that pore sizes can be controlled by flow rate, gas pressure and viscosity of the solution. Recently, a one-step fabrication method of homogenous and scalable porous alginate films was reported in a study,[29] where nitrogen trapped monodispersed alginate microbubbles were obtained through T-junction microfluidics

and the controlled bursting of these after collecting on glass slides. The range of material used in microfluidic fabrication of ordered structures is broad and several additional examples can be found in the literature, including poly lactide-co-glycolide-b-poly ethylene glycol (PLGA-b-PEG), phospholipid, alginate and bovine serum albumin.[21,25,30] Although bubble formation and microfluidic dynamics were well studied, there is a still lack of results related with cell culture experiments in 3D fabricated structures.

In this paper, we demonstrate a novel approach to fabricate 3D gelatin tissue scaffolds with uniform, interconnective pores. Nitrogen gas and gelatin solution without any additional surfactant were pumped through a simple T-junction type microfluidic system and resulting microbubbles were collected at the end of the outlet channel and cross-linked in dilute glutaraldehyde to form 3D biopolymeric foam structures. Factors affecting the microbubble size were investigated in the microfluidic fabrication part and the tissue scaffolds with different pore sizes were characterized in detail, including cell culture studies.

2. Experimental Section

2.1. Microfluidic Setup and Microbubble Characterization

T-type junction apparatus was fabricated by inserting 2 Teflon FEP (Fluorinated Ethylene Polypropylene) capillary tubing perpendicularly into a polydimethylsiloxane (PDMS) block as inlet channels for the flows. Inner diameter of the capillary tubing was 200 µm. A third capillary tube was used as the exit channel of the PDMS block. A controllable infusion pump (NE-1000, New Era Pump Systems, USA) fed gelatin solution and nitrogen flow was maintained and controlled via manometer (Figure 1). A high speed camera (Phantom V7.3, Vision Research Ltd., UK) with a maximum resolution of 800 * 600 pixels at up to 4800 fps recorded the formation of the microdroplets inside the T-junction channel. A video of the microbubble formation is given in SI 1.

5% gelatin solution (Gelatin Type B, Sigma-Aldrich, USA) was used for the fabrication of scaffolds. Briefly, gelatin was completely dissolved in distilled water at 40 °C and the solution was fed into microfluidic channel. The temperature of the experimental environment was monitored via thermometer and kept above 37 °C with the aid of heating gun to avoid gelation of gelatin. Both gelatin and nitrogen flows met at the intersection of the perpendicular channels and microbubble fabrication was carried out. Briefly, gelatin and nitrogen meets at the intersection and gelatin solution penetrates inside the main channel as the nitrogen flow pushes the gelatin droplet and creates a neck. The gelatin neck elongates up to a final length and detaches as a droplet and both gas and liquid phase travels alternately along the channel. As a result, nitrogen entrapped monodispersed microbubbles were collected at the tip-end of the outlet channel. Monodispersity in fabricated microbubbles was investigated by adjusting the flow rate and gas pressure by monitoring via hi-speed camera and a suitable range was achieved in 700 mbar gas pressure. Different flow rates of gelatin solution were used at 700 mbar gas pressure in order to fabricate microbubbles with various diameters. Generated microbubbles were collected either on glass slides or on cylindrical vessels for individual or bulk characterization of the structures. Individual microbubbles cross-linked on glass slides by adding dilute glutaraldehyde solution drops. 3D structures of microbubbles were also collected as scaffolds by immersing the outer tubing into small cylindrical vessels containing varying concentrations of glutaraldehyde (0.25 – 1% (w/v)).

2.2. Characterization of Fabricated Structures

Optical images of microbubbles were collected by optical inverted light microscope (Zeiss Axiotech, Germany) connected via a camera (Nikon Eclipse ME 600, Japan) and diameters of the microbubbles were measured. Uniformity and pore sizes of three dimensional scaffold structures were investigated via scanning electron microscope (SEM, GAIA 3, Tescan, Brno,

Czech Republic). The samples were dried completely and coated for conductivity with Au/Pd sputtering device (ACE600, Leica, Germany) prior to imaging. 3D microbubble structures were also scanned with micro computed tomography (micro CT, Skyscan 1272, Bruker, Germany) to evaluate porosity of scaffold. The porosity calculations were conducted by Bruker CTAn programme. Three cylindrical-shaped independent region of interests (ROI) with approx. 2 mm diameter and 2 mm height were evaluated for each sample group and threshold of ROIs was carried out to obtain binary images. Overall porosity in the scaffolds was calculated by the average 3D porosity values obtained by software.

To investigate the elasticity and shear modulus of the microbubble scaffolds, rheological evaluations were applied with a rotational rheometer (Kinexus Pro, Malvern, United Kingdom). A frequency sweep test (0,1 – 10 Hz) at 1% strain was conducted first to investigate the viscoelastic response of the structures. Subsequently, linear viscoelastic region (LVER) and elastic modulus values of the structures were obtained via strain sweep (1 – 100%) at 1 Hz frequency. During the rheological characterizations scaffolds were kept wet.

Microbubble scaffolds were also investigated for water retention capacity and in vitro hydrolytic degradation. Lyophilized forms of cylindrical structures (6 mm diameter and 10 mm height) were weighed (m_{dry}) and soaked in phosphate buffer saline (PBS) overnight and wet forms were weighed again (m_{wet}). Water retention capacity was calculated by equation below .

$$\text{Water retention capacity} = 100\% \, (m_{wet} - m_{dry}) / m_{dry} \qquad (1)$$

Hydrolytic degradation of the scaffolds was evaluated by immersing the scaffolds in 1 mL PBS at 37 °C and weighing the lyophilized forms at predefined time intervals up to 21 days.

2.3. Cytotoxicity Assay

Effect of cross-linker density on cell viability was quantitatively determined by methylthiazol tetrazolium (MTT) assay according to the ISO 10993-5 standard for in vitro cytotoxicity procedure.

Scaffolds were sterilised by ethanol-PBS washing and UV exposure for 30 min and subsequently soaked in growth medium (89% DMEM, 10% FBS, 1% L-glutamine) for 72 h at 37 °C and 5% CO_2 environment. Meanwhile, L929 mouse fibroblast cells (ATCC, Virginia, USA) were seeded in 96 well plates ($1x10^4$ cells/well) 24 h prior to assay in 5 replicates (n=5). Culture media of cells was replenished with extracted medium from scaffolds (100 µL per well) and allowed to incubate for a further 24 h. Subsequently, pre-warmed 100 µL of 10% MTT reagent contained medium was added into each well and incubated for 3.5 h at 37 °C and 5% CO_2 environment. After incubation all media in sample groups was removed and formazan crystals were dissolved by adding 100 µL dimethyl sulfoxide (DMSO) into each well. Samples were set aside in the dark for half an hour and relative cytotoxicity was determined by measuring the optical density of resulting purple solutions at 570 nm using a multiwall plate reader (Spectramax 190, Molecular Devices, San Jose, CA, USA). 10% DMSO solution containing DMEM and growth medium were used as positive and negative groups, respectively.

2.4. LIVE/DEAD Assay

In order to investigate cellular behaviour such as cell viability, attachment and migration throughout the 3D structures, fluorescence-based LiveDead Cell Viability Assay Kit® (Invitrogen, Paisley, UK) was used. Cylindrical-shaped scaffolds with a diameter of 10 mm and 5 mm height from small, medium and large groups were sterilised with ethanol-PBS washing and UV exposure and subsequently placed on culture flasks containing growth medium for the conditioning of the scaffolds. Following conditioning, L929 cells were cultured on the top of the scaffolds at a density of $1x10^5$ cells/mL and consumed media was replenished 48 h after

cell seeding. On the third day of culture, cell media was withdrawn and scaffolds were rinsed with PBS and subsequently immersed in a solution consisting 2 mM calcein AM and 4 mM ethidium homodimer-1 (EthD-1) in PBS for 45 minutes at 37 °C in the dark. Live (labelled as green) and dead (labelled as red) cells were observed under fluorescence microscopy (Leica Microsystems, Germany).

2.5. Statistical Analysis

Data were expressed as means and standard deviation. Comparison of different groups was performed using the one-way ANOVA test and significant difference was stated if $p < 0.05$.

3. Results and Discussion

Three dimensional biodegradable structures with high porosity have been comprehensively studied as scaffold materials in the tissue engineering both in vitro and in vivo. Pore size and size distribution as well as interconnectivity are critical parameters for cellular bioactivity.[31] Porous character of scaffold material governs the cell penetration, nutrient transport along with degradation profile, mechanical behaviour, angiogenesis and differentiation.[32-34] The influence of pore homogeneity on aforementioned features remains a much lesser studied parameter compared with overall porosity or bulk properties of the scaffold materials. The T-junction microfluidic setup has been used to fabricate microbubbles and particles with a very low polydispersity index.[35-37] In this study, a suitable range for monodispersity was found at 700 mbar gas pressure and flow rates ranging between 50 – 300 µL/min were investigated as the effective parameter on controlling microbubble diameter. For 700 mbar gas pressure, maximum gelatin flow rate was found around 300 µL/min and the resulting gelatin microbubbles had a diameter of 120 µm; however standard deviation was calculated as 12% which indicates poor

monodispersivity. Additionally, because of the higher polydispersity and increasing ratio of the gelatin solution in the mixture, microbubbles did not show a tendency to align as ordered patterns, which means there would be lack of interconnected porosity throughout the resulting structure. Monodispersed bubble with ordered alignment formation was observed between 250 – 100 µL/min flow rates with increasing microbubble diameter and average diameters of the microbubbles were 176±8 µm, 265±9 µm, 286±11 µm and 302±8 µm, respectively. The system was able to generate microbubbles with 50 µL/min flow rate of gelatin solution but the size distribution was very broad indicating that a consistent necking and pinch off stage did not occur due to the high differential between the gas and liquid flows.[38]

Flow rates designate the size of the microbubbles produced in the T-junction process and formation regimes depends on the speed of flow of the two phases. The microbubble formation starts with the entrance of disperse phase in the T-junction area, where the two phases meet. De Menech et al.,[39] investigated the break-up dynamics in a T-junction and proposed three distinct regimes; "squeezing, dripping and jetting". Capillary number (Ca) is defined as the ratio of viscous force and surface tension between two immiscible liquids or liquid/gas interphase and governs the obeyed during droplet formation.[40] Ca is expressed as equation 2;

$$Ca = \mu V / \sigma \qquad (2)$$

where, µ is dynamic viscosity of the fluid, V is fluid velocity and σ is the surface or interfacial tension.[41] The formation obeys the squeezing model at low Ca and changes to dripping and then jetting as Ca increases. In the squeezing regime penetrated fluid breaks into drops and the diameter of the bubble is determined mostly by flow rates but in the dripping regime shear stress exerted by the fluids and pressure take part and Ca becomes more important.[27] Both computational and experimental studies show that the microdroplet/bubble size can be adjusted by varying the flow rates, solution parameters and channel dimensions.[39,42] Here in our study,

Ca can only be changed by V, fluid velocity, as the fluid viscosity and interfacial tensions are fixed since applied gas pressure and solution concentration was kept constant and the drastic decrease in microbubble size at 250-300 µL/min flow rate can be assigned to the start of the dripping regime because of increasing Ca. Figure 2 shows the change of microbubble diameter vs. flow rate and representative images at different stages are shown as insets.

Three different gelatin flow rates (100 µL/min, 200 µL/min and 250 µL/min) were for 3D scaffold fabrication and these groups are denoted as G100, G200 and G250, respectively. A flow rate of 150 µL/min was excluded in the rest of the study because the difference in average diameter was not found statistically significant compared to both 100 and 200 µL/min. Microfluidic bubble formation in T-junction and collected microbubbles are shown in figure 3. Microbubbles generated were cross-linked with glutaraldehyde during collection on glass slides by wetting the surface with cross-linker solution. Three different glutaraldehyde solution (0.25%, 0.5% and 1% (w/v)) were tested for G200 microbubbles to investigate the effect of crosslinking density on size and denoted as G200-025, G200-050 and G200-100, respectively. Glutaraldehyde is a homobifunctional dialdehyde compound and cross-links protein structures by reacting with amino terminated side chains, mostly lysine. The reaction is widely accepted as Schiff base forming and yields one H_2O molecule, resulting in a denser structure. Shrinkage percentages after crosslinking were calculated as 13.7%, 18.4% and 27.2% with respect to increasing glutaraldehyde concentrations. The shrinkage percentage was found to be inversely correlated to the microbubble diameter and calculated as 23.1%, 18.4% and 17.1% for G250-050, G200-050 and G100-050 sample groups, respectively. The effect of cross-linker concentration was found more influential on size decrease compared to bubble size since the amount of reactive aldehyde functionality per unit area was higher than for the other sample groups containing lower amounts of cross-linker.

3D microbubble scaffold structures were collected by immersing the outer tubing into small cylindrical vessels. Bubble structures liberated from outer end travel upwards along the vessel

containing varying concentrations of glutaraldehyde and stacked on top. Gelatin microbubble scaffold formation is shown as SI 2.

Obtained 3D structures were removed from vessels and dried in open air for the observation in SEM and micro CT analysis. Scaffolds with varying diameters were cut and sectioned with a sharp razor and investigated under SEM after gold coating. Cross-section observation of scaffolds showed that pores emerged as a result of bursting of microbubbles and exhibit homogeneity in each group (Figure 4a-e). The sizes of pores show similar values with microbubble diameters in groups. Additionally, multiple interconnection of pores generated at contact points of microbubbles indicate a well-established porous interconnected network structure. Interconnectivity in porous scaffolds is a crucial feature in tissue engineering and regenerative medicine. Diameters of these pores were measured between 15 – 80 µm, which is a suitable range for both nutrient media transportation and as well as cell migration[32,43,44]. Moreover, the role of interconnectivity in 3D scaffolds has been studied in detail and optimal pore size for vascularization was found around 40 µm.[45,46] Somo et al.,[6] have found that in an in vivo trial interconnectivity with even larger pores in hydrogel tissue scaffold allows more vascularization and blood vessel networks, 3-6 weeks after implantation. Thickness of the pore wall struts was found to be 5 µm in all samples with a few structural differences. Scaffolds generated using the smallest microbubbles or the highest crosslinking concentration (1%) exhibit wrinkles on the pore walls, which can be caused by higher shrinkage ratio above 20%. Besides, three-dimensional structures obtained with 0.25% glutaraldehyde looks much loose than the other groups, indicating crosslinking at this rate generates softer scaffolds with less interconnected pores.

Figure 5 shows the reconstructed 3D images of the sample groups obtained by micro-tomography scanning. All gelatin scaffolds represent similar macrostructures, consisting of well interconnected spherical pores. The insets show both representative macro and interconnection pores. The calculated total porosity of all samples ranged between 65 – 81%

and also an increase in microbubble diameter resulted in higher porosity. The relevant data are summarized in Table 1.

The rheological behaviour of the (see graph in SI 3) three-dimensional hydrogel scaffolds were evaluated with frequency sweep between 0.1 – 10 Hz and at 1% constant strain. The change in elastic (G') and viscous (G'') moduli as a function of frequency are shown in these graphs which revealed that rheological behaviour of all the scaffolds are similar to viscoelastic gel material since both elastic and viscous moduli are independent of the frequency. Moreover, G' values are at least one order of magnitude higher than G'' values in all the samples with a low phase angle (< 5°). The effects of microbubble size and glutaraldehyde concentration on elasticity were also investigated with strain sweeps (1 – 100%) at 1 Hz frequency (figure 6 a-c). Both linear viscoelastic region and elastic modulus values are found to be decreasing with increasing bubble size as previously reported.[47] This finding is also related to the porosity values, since larger voids are present with increasing bubble size. The elastic modulus for G250-050, G200-050 and G100-050 scaffolds at 10% strain were calculated as 770, 620 and 440 Pa, respectively. The change in elastic modulus is much more notable in cross-linker density evaluation as can be seen in figure 6b. G' value for G200-025 scaffolds exhibits a resemblance to the G200-050 group, while it exceeds 1 kPa for G200-100. Beside elastic modulus, the longest linear viscoelastic region is observed in the 0.25% cross-linked samples which correlates well with the above-mentioned SEM findings, indicating the loosest network amongst the sample groups.

Water retention results of gelatin scaffolds are given in figure 6d. Scaffolds with higher porosities with same crosslinking ratios exhibit less retention capacities compared to lower porosity samples. This indicates that swelling of scaffolds is inversely correlated to porosity and water absorption occurs inside the hydrophilic gelatin network rather than void volume. The relationship between crosslinking and water uptake was found concordant with findings in literature[48,49] Low crosslinking density significantly increased the water uptake up to 1100%,

whereas 700% swelling was recorded with 1% glutaraldehyde concentration. Swelling of a tissue scaffold material plays a key role, both *in vivo* and *in vitro*. The water uptake allows nutrients and other biomolecules transport along the tissue scaffold through interconnected pores or diffusion via polymer walls.[50] On the other hand, water retention capacity under physiological conditions must be optimized; otherwise, excessive swelling may end up with rapid degradation before the extracellular matrix secretion and tissue development. The graph in figure 6e verifies the relation between water retention and the hydrolytic degradation and shows the mass loss of scaffolds in 21 days under physiological conditions. G200-025 sample group, which has the lowest crosslinking ratio, rapidly degrades and loses its 41% of weight at the end of first week and completely dissolves in aqueous media after 21 days. The rest of the scaffolds exhibit similar trends in accordance with swelling data. G100-050, G200-050 and G250-050 sample groups preserve 38%, 51% and 61% of their mass after 21 days, respectively; whereas G200-100 group loses only 24% of mass during the hydrolytic degradation. The secretion of extracellular matrix components, consisting of distinct biomolecules begins at various stages in tissue formation. Scaffolds as a support material for cells must be intact and convenient for cells to adhere for the steady progress of tissue growth. Hence, scaffold material integrity is crucial in the early development phase before ECM synthesis. Many studies have shown that the genes responsible for the synthesis of differentiation markers, generally upregulate after 2 weeks following cell seeding.[51,52]. Additionally, vascular tissue development is only possible with the adequate amounts of ECM proteins, collagen and elastin.[53]

To investigate the cytotoxicity, cell attachment, infiltration through the scaffold, both MTT and LIVE/DEAD Cell Viability assays were performed. Fig 7a-e shows representative fluorescence microscopy images of data obtained from each sample group, where green fluorescence indicates live and red fluorescence indicates dead cells. In sample groups, dead cells were only observed in G200-100 sample group, which was cross-linked with 1% glutaraldehyde solution.

This result also correlates with the MTT assay, (figure 7f), where % viability of the G200-100 group was below 70%. At lower concentrations of glutaraldehyde, cell viability values were above 90%. Concordantly, the abundancy of attached live cells in figure 7a-d indicates high cell viability amongst scaffolds. It is known that, mean pore size can directly affect cellular behaviour such as cell adhesion, ensuing proliferation, migration and infiltration.[54] Our results demonstrated that, among fabricated scaffolds, the highest cell viability was observed in the G200-050 group with considerably more cell attachment which means that mean pore size is crucial for higher cell attachment and growth. In some regions of the fluorescence images, circular organizations of live cells were remarkable, showing that cell localization pattern is governed by fabricated structure Moreover, in each sample group green cell signals were observed in different layers, indicating that cells infiltrated through the scaffold during culture. This evidence supports the hypothesis and previous visual findings that scaffolds originated from microbubbles are well-interconnected and keeps their network through the cell culture, which allows cell hosting all around the structure during the tissue development stage.

4. Conclusions

Controlling pore size and uniform porosity is a crucially important issue in scaffold design since it is a fundamental feature which effects cell growth, migration, nutrient transport, mechanical properties and differentiation. In this study, we fabricated gelatin scaffolds having homogeneous pore diameter with a narrow size distribution using a T-junction microfluidic bubbling system. The method is simple, rapid and inexpensive. The pore size of the resultant scaffolds was determined by the bubble diameter which was controlled precisely by flow parameters. High porosity and interconnectivity were observed in all sample groups. Moreover, viscoelasticity and degradation profiles were also analysed. Mouse fibroblast cells attached, proliferated and penetrated through the scaffold without receiving any cytotoxic effect in low

density cross-linked samples. The study emphasizes that scaffolds made of microbubbles generated by microfluidics can be used in further tissue engineering and cell encapsulation applications especially in pore size dependent studies.

Supporting Information

Supporting Information is available from the Wiley Online Library or from the author.

Acknowledgements

This study was supported by Hacettepe University, Scientific Research Projects Coordination Unit Grant No: FBI-2017-14296. CB and XJ contributed equally to this work.

Conflict of Interest

The authors declare no conflict of interest.

Keywords: biofabrication, gelatin, tissue scaffold, microbubble

Received: ((will be filled in by the editorial staff))
Revised: ((will be filled in by the editorial staff))
Published online: ((will be filled in by the editorial staff))

References

[1] K. M. Ye, D. L. Kaplan, G. Bao, C. Bettinger, G. Forgacs, C. Dong, A. Khademhosseini, Y. G. Ke, K. Leong, A. Sambanis, W. Sun, P. Yin, *ACS Biomater. Sci. Eng.*, **2018**, *4*, 2292-2307.

[2] A. H. Morris, H. Lee, H. Xing, D. K. Stamer, M. Tan, T. R. Kyriakides, *ACS Appl. Mater. & Inter.*, **2018**, *10*, 41892-41901.

[3] O. A. Chanes-Cuevas, A. Perez-Soria, I. Cruz-Maya, V. Guarino, M. A. Alvarez-Perez, *AIMS Mater. Sci.*, **2018**, *5*, 1124-1140.

[4] N. Arabi, A. Zamanian, S. N., Rashvand, F. Ghorbani, *Macromol. Mater. Eng.*, **2018**, *303*, 1700539.

[5] D. Puppi, A. Morelli, F. Bello, S. Valentini, F. Chiellini, *Macromol. Mater. Eng.*, **2018**, *303*, 1800247.

[6] S. I. Somo, B. Akar, E. S. Bayrak, J. C. Larson, A. A. Appel, H. Mehdizadeh, A. Cinar, E. M. Brey, *Tissue Eng. Part C Methods*, **2015**, *21*, 773-785.

[7] D. R. Fonseca, R. Sobreiro-Almeida, P. C. Sol, N. M. Neves, *Macromol. Mater. Eng.*, **2019**, *304*, 1800623.

[8] F. J. O'Brien, *Mater. Today*, **2011**, *14*, 88-95.

[9] H. M. Aydin, A. J. El Haj, E. Piskin, Y. Yang, *J. Tissue Eng. Regen. Med.*, **2009**, *3*, 470-476.

[10] Q. L. Loh, C. Choong, *Tissue Eng. Part B, Reviews*, **2013**, *19*, 485-502.

[11] B. Dhandayuthapani, Y. Yoshida, T. Maekawa, D. S. Kumar, *Int. J. Polym. Sci.*, **2011**, *19*, 290602.

[12] N. Kasoju, N. Hawkins, O. Pop-Georgievski, D. Kubies, F. Vollrath, *Biomater. Sci.*, **2016**, *4*, 460-473.

[13. I. Manavitehrani, T. Y. L. Le, S. Daly, Y. W. Wang, P. K. Maitz, A. Schindeler, F. Dehghani, *Mater. Sci. Eng. C-Mater. Biol. Appl.*, **2019**, *96*, 824-830.

[14] L. Y. Xiao, C. H. Zhu, Z. Z. Ding, S. S. Liu, D. Y. Yao, Q. Lu, D. L. Kaplan, *J. Mater Chem. B*, **2018**, *6*, 4308-4313.

[15] Y.Z. Wan, T. Cui, Q.C. Zhang, Z.W. Yang, F.L. Yao, H.L. Luo, *Macromol. Mater. Eng.*, **2018**, *303*, 1800316.

[16] S.F. Liu, Y. Hu, J.C. Zhang, S.Q. Bao, L. Xian, X.M. Dong, W.X. Zheng, Y.H. Li, H. C. Gao, W. Y. Zhou, *Macromol. Mater. Eng.*, **2019**, *304*, 1800698.

[17] A. Wubneh, E. K. Tsekoura, C. Ayranci, H. Uludag, *Acta Biomater.*, **2018**, *80*, 1-30.

[18] E. Fantino, I. Roppolo, D. X. Zhang, J. F. Xiao, A. Chiappone, M. Castellino, Q. Q. Guo, C. F. Pirri, J. Yang, *Macromol. Mater. Eng.*, **2018**, *303*, 1700356.

[19] P. Ravi, P. S. Shiakolas, T. R. Welch, *Addit. Manuf.*, **2017**, *16*, 167-176.

[20] M. Karimpoor, E. Yebra-Fernandez, M. Parhizkar, M. Orlu, D. Craig, J. S. Khorashad, M. Edirisinghe, *J. R. Soc. Interface*, **2018**, *15*, 8.

[21] Z. Ekemen, H. Chang, Z. Ahmad, C. Bayram, Z. M. Rong, E. B. Denkbas, E. Stride, P. Vadgama, M. Edirisinghe, *Biomacromolecules*, **2011**, *12*, 4291-4300.

[22] X. F. Liu, P. Gong, P. F. Song, F. Xie, A. L. Miller, S. G. Chen, L. C. Lu, *Biomater. Sci.*, **2018**, *6*, 623-632.

[23] Y. J. Ho, T. C. Wang, C. H. Fan, C. K. Yeh, *ACS Appl. Mater. Inter.*, **2018**, *10*, 17784-17791.

[24] Z. Ekemen, Z. Ahmad, E. Stride, D. Kaplan, M. Edirisinghe, *Biomacromolecules*, **2013**, *14*, 1412-1422.

[25] M. Gultekinoglu, X. Jiang, C. Bayram, K. Ulubayram, M. Edirisinghe, *Langmuir*, **2018**, *34*, 7989-7997.

[26] T. Glawdel, C. Elbuken, C. L. Ren, *Phys Rev E Stat Nonlin Soft Matter Phys*, **2012**, *85*, 016322.

[27] P. Garstecki, M. J. Fuertsman, H. A. Stone, G. M. Whitsides, *Lab Chip*, **2006**, *6*, 437-446.

[28] K. Y. Chung, N. C. Mishra, C. C. Wang, F. H. Lin, K. H. Lin, *Biomicrofluidics*, **2009**, *3*, 8.

[29] M. Elsayed, A. Kothandaraman, M. Edirisinghe, J. Huang, *Langmuir*, **2016**, *32*, 13377-13385.

[30] K. P. Pancholi, U. Farook, R. Moaleji, E. Stride, M. J. Edirisinghe, *Eur. Biophys. J. Biophys. Lett.*, **2008**, *37*, 515-520.

[31] V. Karageorgiou, D. Kaplan, *Biomaterials*, **2005**, *26*, 5474-5491.

[32] K.-H. Wu, C. Mei, C.-W. Lin, K.-C. Yang, J. Yu, *J. Mater. Chem. B*, **2018**, *6*, 125-132.

[33] E. H. Song, Y. J. Seong, J. Kim, H. E. Kim, S. H. Jeong, *Macromol. Mater. Eng.*, **2019**, *304*, 1800352.

[34] Z. J. Wang, H. Kumar, Z. L. Tian, X. Jin, J. F. Holzman, F. Menard, K. Kim, *ACS Appl. Mater.Inter.*, **2018**, *10*, 26859-26869.

[35] D. Vecchiolla, V. Giri, S. L. Biswal, *Soft Matter*, **2018**, *14*, 15.

[36] X. Jiang, Y. Zhang, M. Edirisinghe, M. Parhizkar, *RSC Adv.*, **2016**, *6*, 63568-63577.

[37] M. Parhizkar, E. Stride, M. Edirisinghe, *Lab Chip*, **2014**, *14*, 2437-2446.

[38] A. Kothandaraman, A. Harker, Y. Ventikos, M. Edirisinghe, *Micromachines*, **2018**, *9*, 19.

[39] M. De Menech, P. Garstecki, F. Jousse, H. Stone, *J.Fluid Mech.*, **2008**, 595, 141-161.

[40] C. N. Baroud, F. Gallaire, R. Dangla, *Lab Chip*, **2010**, *10*, 2032-2045.

[41] J. Xu, S. Li, J. Tan, G. Luo, *Microfluid. Nanofluidics*, **2008**, *5*, 711-717.

[42] G. F. Christopher, N. N. Noharuddin, J. A. Taylor, S. L. Anna, *Phys. Rev. E*, **2008**, *78*, 036317.

[43] S. J. Hollister, *Nature Materials*, **2005**, *4*, 518.

[44] E. Babaie, S. B. Bhaduri, *ACS Biomater. Sci. Eng.*, **2018**, 4, *1*-39.

[45] A. Galperin, T. J. Long, B. D. Ratner, *Biomacromolecules*, **2010**, *11*, 2583-2592.

[46] L. R. Madden, D. J. Mortisen, E. M. Sussman, S. K. Dupras, J. A. Fugate, J. L. Cuy, K. D. Hauch, M. A. Laflamme, C. E. Murry, B. D. Ratner, *Proc. Natl. Acad. Sci. USA*, **2010**, *107*, 15211-15216.

[47] A. Borzacchiello, L. Mayol, P. A. Ramires, A. Pastorello, C. Di Bartolo, L. Ambrosio, E. Milella, *Biomaterials*, **2007**, *28*, 4399-4408.

[48] G. Yang, Z. Xiao, H. Long, K. Ma, J. Zhang, X. Ren, J. Zhang, *Sci. Rep.*, **2018**, *8*, 1616.

[49] X. Zhao, X. Sun, L. Yildirimer, Q. Lang, Z. Y. Lin, R. Zheng, Y. Zhang, W. Cui, N. Annabi, A. Khademhosseini, *Acta Biomater.*, **2017**, *49*, 66-77.

[50] K. Maji, S. Dasgupta, K. Pramanik, A. Bissoyi, *Inter. J. Biomater.* , **2016**, 9825659.

[51] X. Wang, Z. Chen, B. Zhou, X. Duan, W. Weng, K. Cheng, H. Wang, J. Lin, *ACS Appl. Mater. Inter.*, **2018**, *10*, 11508-11518.

[52] X. Y. Peng, M. Hu, F. Liao, F. Yang, Q. F. Ke, Y. P. Guo, Z. H. Zhu, *Biomater. Sci.*, **2019**, ***7***, 1565-1573.

[53] F. F. R. Damanik, C. van Blitterswijk, J. Rotmans, L. Moroni, *J. Mater. Chem. B*, **2018**, *6*, 6468-6480.

[54] C. M. Murphy, F. J. O'Brien, *Cell Adhes Migr.*, **2010**, *4*, 377-381.

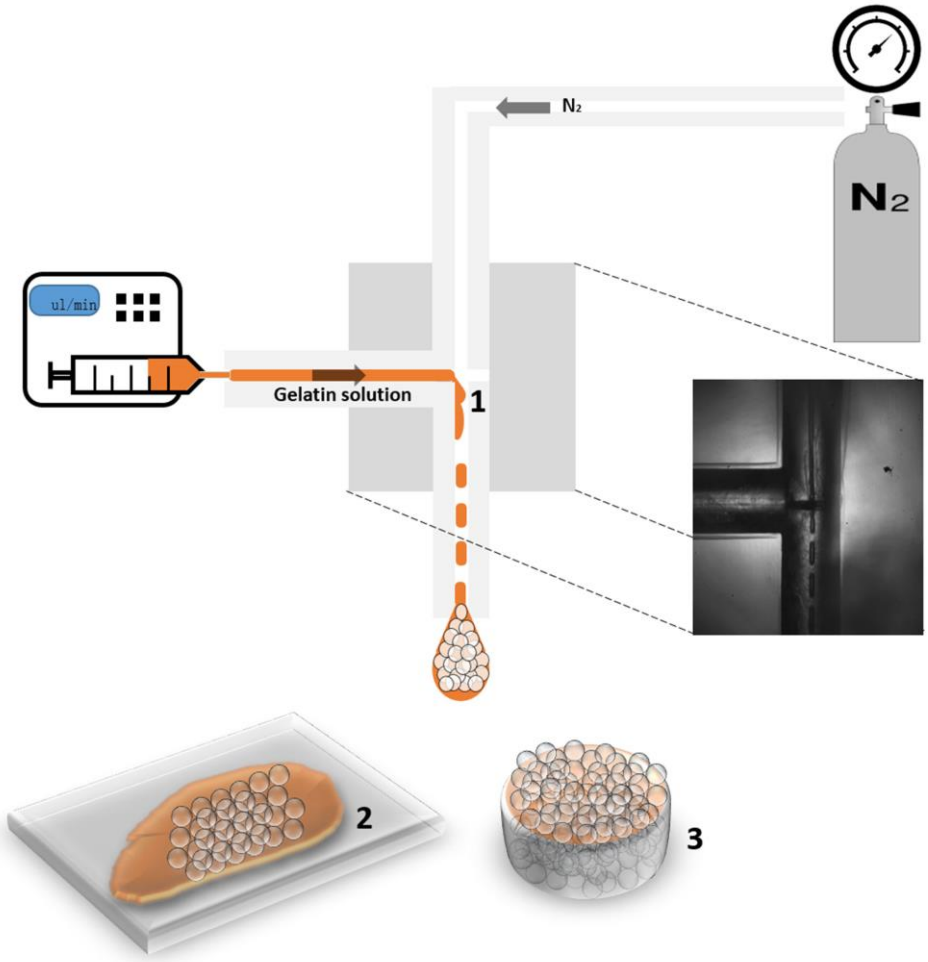

Figure 1. Schematic representation of microbubble fabrication with T-junction microfluidics. Two phases meet at the T-junction and microbubble formation is established (1). Gelatin microbubbles are collected on either glass slides (2) or small vessels (3) in 2D or 3D configuration, respectively.

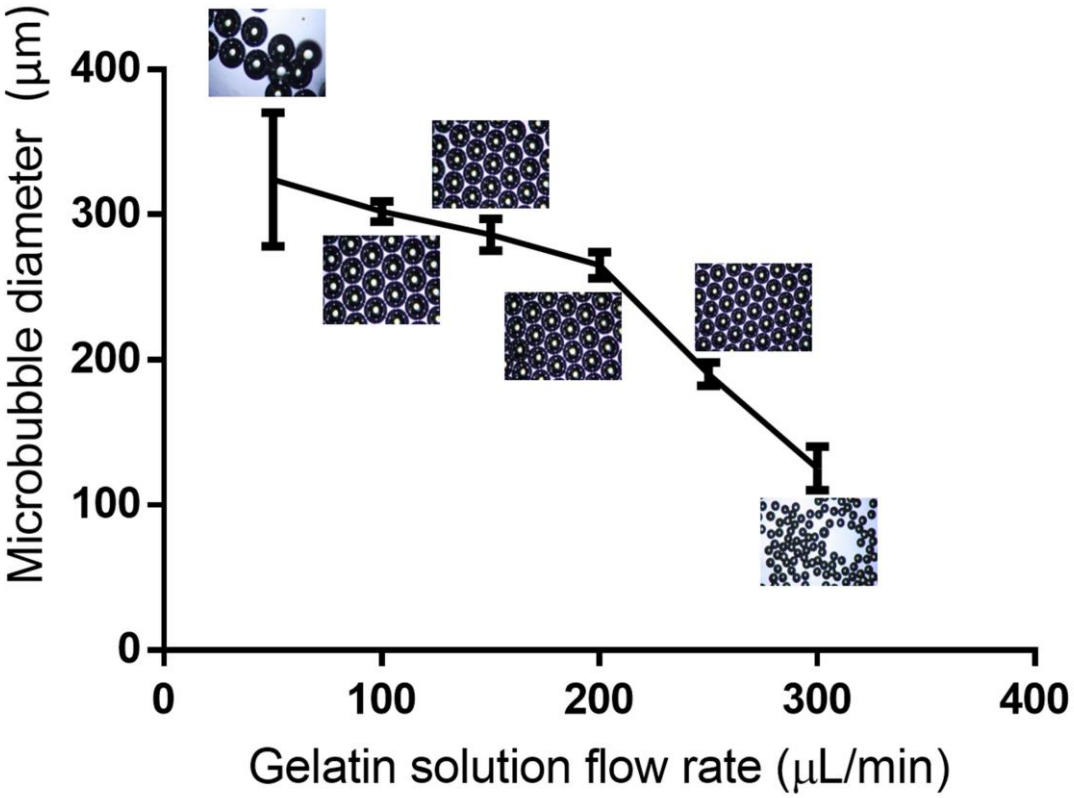

Figure 2. Microbubble diameter – gelatin solution flow rate relationship.

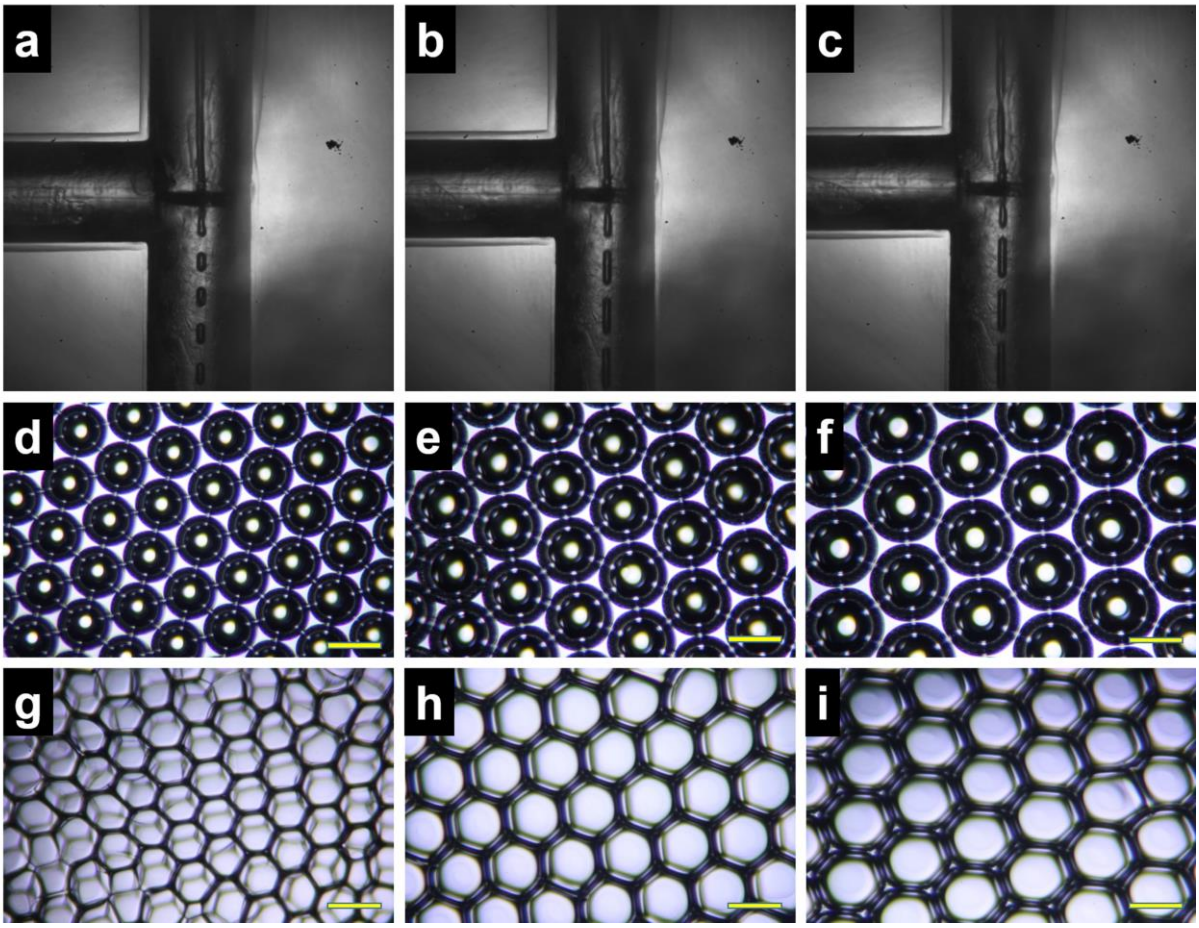

Figure 3. Microbubble generation in G250, G200 and G100 groups. High speed camera images of G250 (250 µL/min), G200 (200 µL/min) and G100 (100 µL/min) of bubble generation (a-c). Microbubble array formation immediately after collection on glass slides (d-f). Burst and shrunk microbubble arrays after crosslinking (g-i). Scale bars show 100 µm.

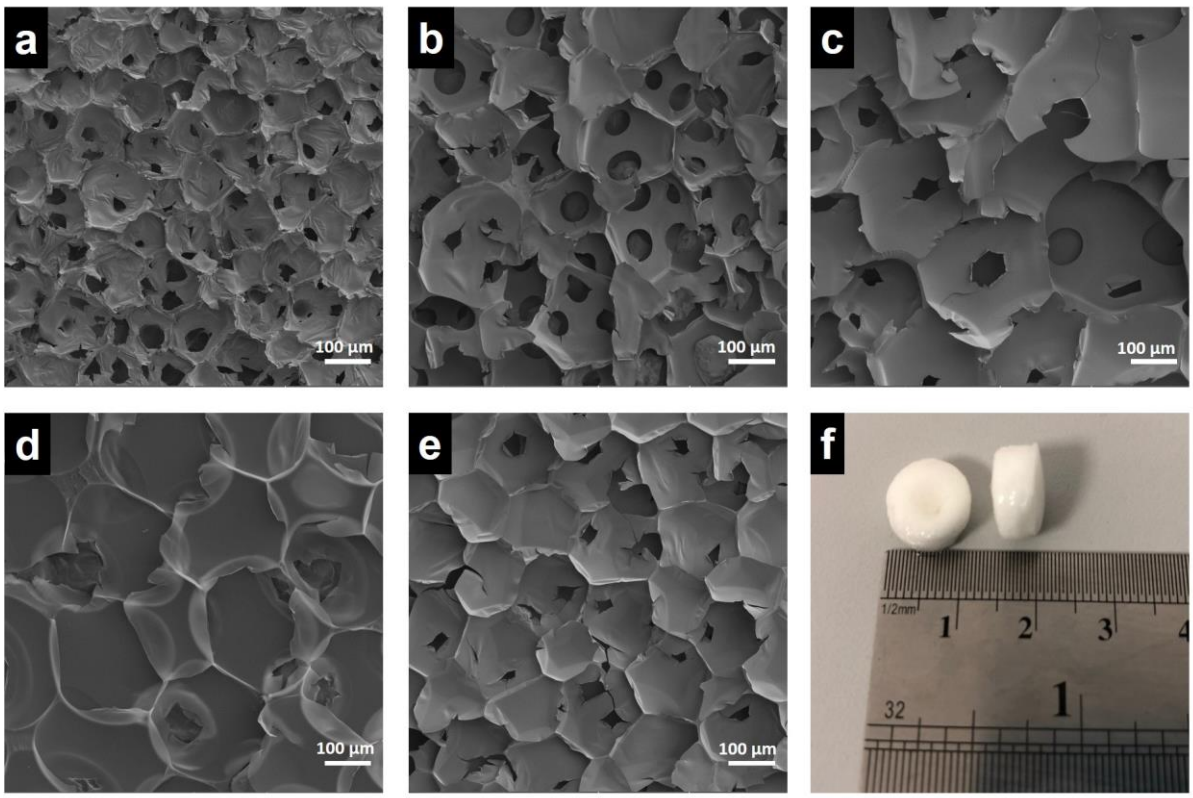

Figure 4. SEM images of the samples obtained with different flow ratios (G250-050, G200-050 and G100-050) (a-c) and cross-linked with different concentrations of glutaraldehyde (G200-025 and G200-100) (d-e). Pore diameter increases with decreasing gelatin flow rate and cross-linking concentrations. Interconnectivity is established in each sample. White bar indicates 100 µm. Representative samples for 3D microbubble scaffold (f).

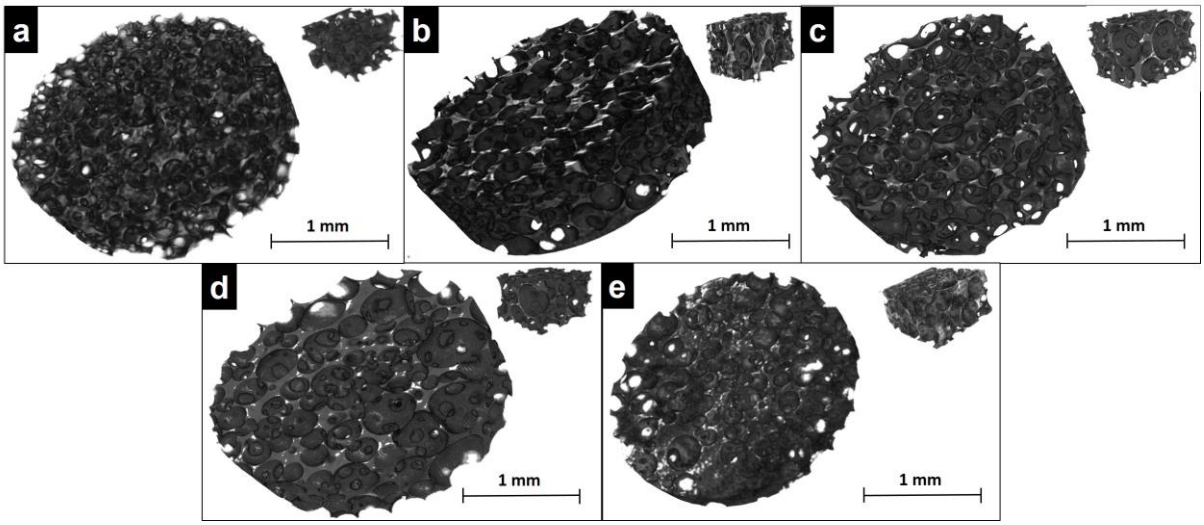

Figure 5. Reconstructed micro-tomography images of scaffolds prepared using gelatin microbubbles. Upper row shows different flow ratios (G250-050, G200-050 and G100-050) (a-c) and lower row shows structures cross-linked with different concentrations of glutaraldehyde cross-linking (G200-025 and G200-100) (d-e). Insets shows the random interior volumes; interconnectivity is well-established in each sample group.

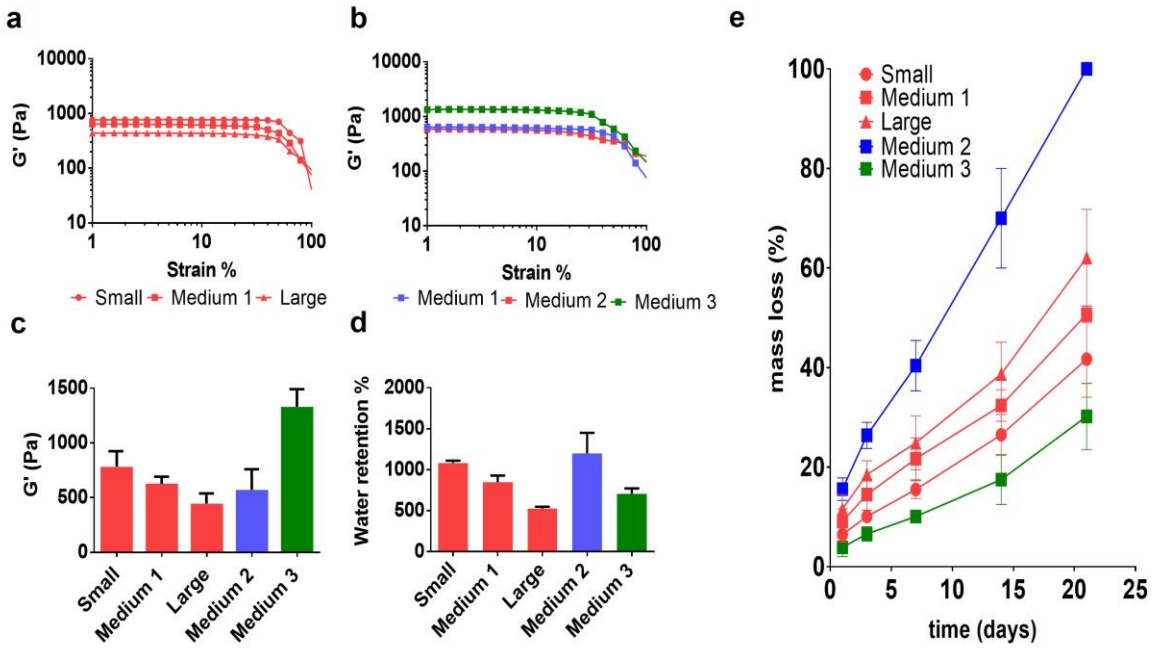

Figure 6. Viscoelastic and degradation properties of microbubble scaffolds. Strain sweeps (a-b); storage moduli (c); water retention capacity (d) and degradation profiles (e).

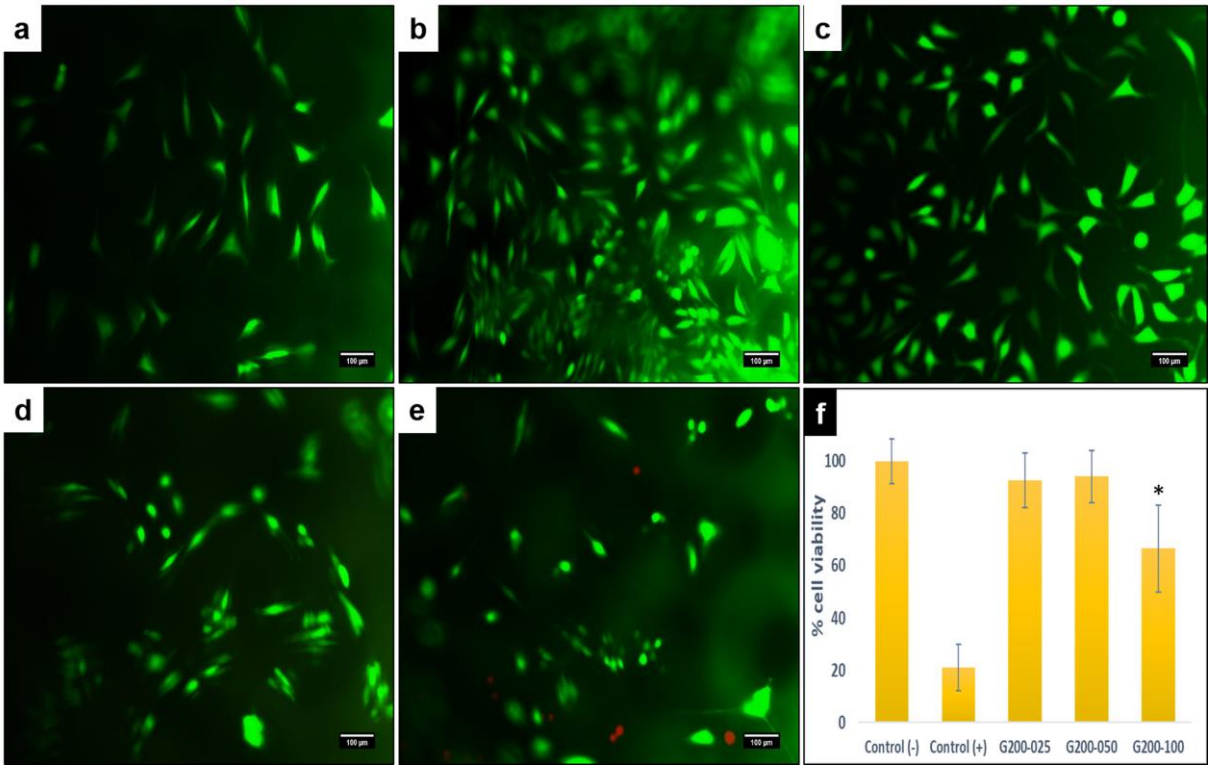

Figure 7. Cytotoxicity investigations of gelatin microbubble scaffolds. Fluorescence microscopy images of G250-050, G200-050, G100-050, G200-025 and G200-100 samples, respectively (a-e) and indirect cytotoxicity evaluations of crosslinking density, * indicates significant difference ($p < 0.05$) (f). (Scale bars: 100 µm)

Table 1. Summary of pore diameter (μm) and porosity values of the scaffolds prepared

	Diameter before cross-linking	Glutaraldehyde %	Diameter after cross-linking	Shrinkage %	Porosity of 3D structure %
G250-050	*176±8*	*0.5*	*135±11*	*23.1*	*65.6*
G200-050	*265±9*	*0.5*	*216±9*	*18.4*	*76.8*
G100-050	*302±8*	*0.5*	*250±12*	*17.1*	*81.4*
G200-025	*265±9*	*0.25*	*231±5*	*13.1*	*80.3*
G200-100	*265±9*	*1*	*193±11*	*27.2*	*69.0*

Table of Contents

Uniform porosity is a fundamental feature affecting cell growth, migration, mechanical properties and cell differentiation. Gelatin scaffolds having homogeneous pore diameter with a narrow size distribution were fabricated using a T-junction microfluidic bubbling system. The method is simple, rapid and inexpensive. This study emphasizes that scaffolds made by bottom-up assembly of uniform microbubbles can be used in a wide range of applications, especially in pore size dependent studies.

Cem Bayram†, Xinyue Jiang†, Merve Gultekinoglu, Sukru Ozturk, Kezban Ulubayram and Mohan Edirisinghe*

Biofabrication of gelatin tissue scaffolds with uniform pore size via microbubble assembly

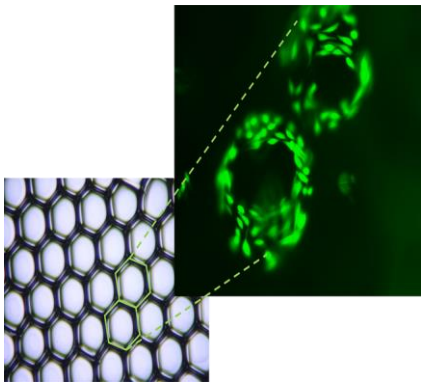

ToC figure

Supporting Information

Biofabrication of gelatin tissue scaffolds with uniform pore size via microbubble assembly

Cem Bayram†, Xinyue Jiang†, Merve Gultekinoglu, Sukru Ozturk, Kezban Ulubayram and Mohan Edirisinghe*

Supplementary Information 1. Microbubble formation inside T-junction channel.

Supplementary Information 2. Gelatin microbubble scaffold formation.

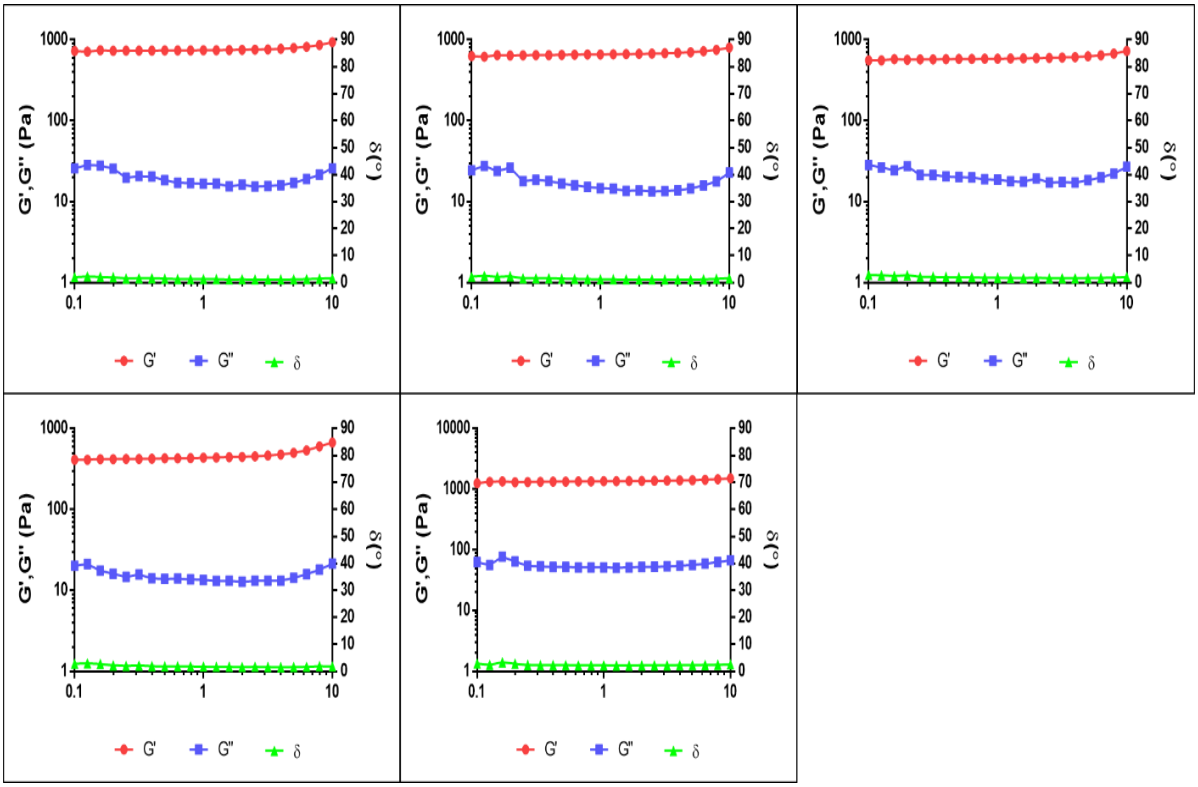

Supplementary Information 3. Frequency sweeps of gelatin microbubble scaffolds created with different flow ratios (250-200-100 µL/min, 0.50% glutaraldehyde) (a-c) and cross-linked with different concentrations of glutaraldehyde (200 µL/min, 0.25 and 1% glutaraldehyde) (d,e). The graphs revealed that rheological behaviour of all scaffolds are similar to those of viscoelastic gel material since both elastic and viscous moduli are frequency independent. Moreover, *G'* values are at least one order of magnitude higher than *G''* values in all samples with a low phase angle (< 5°).

MS incl figures, tables w/o highlighted area

Short summary

TOC image


Click here to access/download
Production Data
TOC_55x50.png

Figure 1

Click here to access/download

Production Data

Fig 1.tif

Figure 2

Click here to access/download

Production Data

Fig 2.tif

Figure 3

Click here to access/download

Production Data

Fig 3.tif

Figure 4

Click here to access/download

Production Data

Fig 4.tif

Figure 5

Click here to access/download

Production Data

Fig 5.tif

Figure 6

Click here to access/download

Production Data

Fig 6.tif

Figure 7

Click here to access/download

Production Data

Fig 7.tif

Supporting Information 1 video

Click here to access/download

Production Data

SI 1.mp4

Supporting Information 2 video

Click here to access/download

Production Data

SI 2.mp4

Supporting Information 3 docx